

Effects of Cu on the crystallization behaviour of amorphous $\text{Fe}_{71}\text{Cr}_{15}\text{Mo}_4\text{B}_{10}$

R.G. VARDIMAN, J.D. AYERS, H.N. JONES

Physical Metallurgy Branch, Code 6321, Naval Research Laboratory, Washington, DC 20375-5343 USA

Following the approach of earlier studies which have demonstrated that nanocrystalline microstructures can be produced in soft magnetic alloys through the addition of one percent of Cu to Fe based amorphous precursor alloys, it is demonstrated that substantial grain refinement can be produced in alloys of interest for structural applications. Grain sizes of approximately 50 nm were produced in the alloy $\text{Fe}_{70}\text{Cr}_{15}\text{Mo}_4\text{B}_{10}\text{Cu}_1$. Such grain sizes should permit superplastic consolidation of powder or flake at reasonable rates with moderate die pressures at temperatures in the vicinity of 650 °C.

1. Introduction

There has long been an interest in the metallurgical community in methods for refining the microstructure of crystalline alloys. Traditional methods such as warm and cold working can easily generate grain sizes as small as a few micrometres, but only in special cases can they produce grains with all dimensions below one micrometre. Grain sizes well below one micrometre are sometimes produced when amorphous metals are crystallized, but sizes vary substantially with the glass composition and the crystallization temperature. Yoshizawa and co-workers [1] employing the observations of Masumoto *et al.* [2] that small additions of Cu, Ag and Au to amorphous alloys can lead to the formation of nanometre-scale crystallites during melt quenching, found that additions of about 1% Cu could induce the nucleation of Fe-rich b.c.c. crystallites only a few nanometres in size during the heat treatment of amorphous Fe–Si–B alloys. When they also added small amounts of Nb to the alloys, Yoshizawa and co-workers were able to produce an alloy containing b.c.c. crystallites about 10 nm in diameter, these being separated by a thin residual film of amorphous material, and this composite structure exhibited superior soft magnetic properties [1, 3, 4]. Similarly, Suzuki *et al.* [5] found that adding 1% Cu to an amorphous Fe–Zr–B alloy reduced the grain size of the crystallized material to a few nanometres and improved the soft magnetic properties. This refinement in structure has been attributed [1, 6] to the Cu-inducing compositional modulations in the crystallizing material which stimulates nucleation at the b.c.c. phase on a fine scale. Ayers and colleagues [7] found, in an extended X-ray absorption fine structure (EXAFS) study of the Fe–Si–B based alloys of Yoshizawa *et al.*, that small Cu clusters with near-f.c.c. symmetry form very early in the crystallization process, and they hypothesized that these clusters catalyse precipitation of the b.c.c. nanocrystals.

The experiments reported here were directed toward determining whether minor additions of Cu could refine the microstructures of crystallized amorphous alloys which have potential interest for structural applications. Such a refinement might increase the strength of the alloys or make them amenable to superplastic forming. Superplastic forming rates are expected to increase rapidly with decreasing grain size because the creep rate increases as the inverse square or inverse cube of the grain diameter, depending on whether lattice diffusion or grain boundary diffusion is rate controlling (see, for example, Sherby and Wadsworth [8]).

It was considered desirable to do this investigation on materials which might be expected to exhibit attractive mechanical properties after appropriate processing, but, while amorphous metals have long been touted as attractive precursors for the formation of fine-grained crystalline alloys for structural applications, we are aware of only one class of such materials having come into commercial use. These are the Devitrium® alloys developed by Ray [9] for Allied-Signal and marketed by Amax Speciality Metals. Most metallic alloys which can be made amorphous by rapid solidification contain one or more elements, used to prevent crystallization during solidification, which induce the formation of hard, brittle phases in the crystallized alloy. These brittle phases are generally present in sufficient quantity to be deleterious to the properties of the crystallized alloys. The Fe- and Ni-based alloys developed by Ray use B as the primary glass former, but they have acceptable amounts of the hard boride phases after crystallization because transition metals such as Cr and Mo are substituted for some of the B which is normally needed to suppress crystallization during melt quenching of Fe and Ni alloys. The base alloy selected for study here is one of the simpler ones reported by Ray. It has the composition $\text{Fe}_{71}\text{Cr}_{15}\text{Mo}_4\text{B}_{10}$. This paper reports only on

microstructural effects, for mechanical properties have not yet been investigated.

The ternary phase diagrams for Fe–Cr–Mo [10], Fe–Cr–B [11], Fe–Mo–B [12, 13] and Cr–Mo–B [14] suggest that the equilibrium phase structure for the alloy used here should be primarily α -Fe solid solution with some χ (Fe–Cr–Mo) phase and either Cr_2B or Fe_2B or possibly both. Both borides have extensive solubility for the other metallic components; in fact, Cr_2B can contain more iron than chromium [11]. In addition, Fe_3B , which is metastable below 1150 °C [15], is known to form during crystallization of rapidly quenched Fe–B alloys such as $\text{Fe}_{80}\text{B}_{20}$ [15, 16].

We used transmission electron microscopy (TEM) and selected area electron diffraction (SAD) to identify the principal phases and grain morphology in the alloys studied here. Electron diffraction is much more sensitive than X-ray diffraction to the early stages of precipitation and can identify phases more readily where small precipitate size causes broadening of X-ray peaks. Phase development was followed after heat treatment between 400 and 850 °C.

2. Experimental methods

Alloys of atomic compositions $\text{Fe}_{71}\text{Cr}_{15}\text{Mo}_4\text{B}_{10}$ and $\text{Fe}_{71}\text{Cr}_{15}\text{Mo}_4\text{B}_{10}\text{Cu}_1$ were prepared from metals of 99.99% purity or better by arc melting on a chilled Cu hearth in an argon atmosphere. Rapidly solidified ribbons, 20–25 mm thick and 1.5–2 mm wide, were prepared by inductively melting the alloys in fused quartz under He gas and ejecting the melt from a fine orifice onto the perimeter of a Cu wheel rotating at a surface speed of 48 ms^{-1} . Sections of the ribbon samples were sealed in glass capsules under half an atmosphere of He and heat treated at temperature for 60 min.

Because the ribbons were substantially less than 3 mm in width, they were more suited to thinning for TEM by ion milling than by electrochemical polishing. For support and protection of the sides they were first mounted with epoxy on a copper grid with a 1 × 2 mm slot. Ion milling was performed at 4 keV at an 18° angle, reduced to 3 keV at 12° in the final stage. No evidence of damage from milling was observed.

The phases present were identified by selected area electron diffraction. As the α -iron phase was prominent in most cases, its diffraction rings were used whenever possible to calibrate the diffraction pattern.

3. Results

The alloy without Cu remains amorphous after heat treatment at 400 °C, and shows only a fine precipitate of the χ phase at 475 °C (Fig. 1). At 550 °C full recrystallization has occurred with the appearance of the α -Fe solid solution and the metastable Fe_3B along with the χ phase. The Fe_3B grains are large compared to other grains observed here (Fig. 2), of the order of 300 to 500 nm, and their irregular appearance suggests they were from the last of the amorphous material to crystallize. This phase mixture appears the same after heat treatment at 700 °C, but the Fe_3B grains are

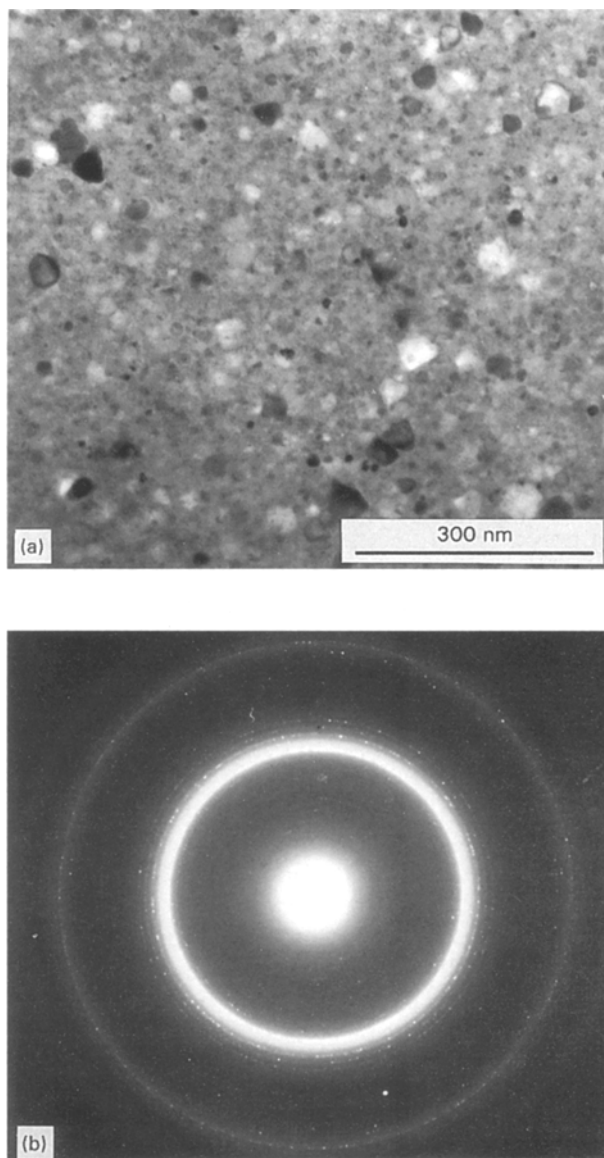


Figure 1 Base alloy, 1 h at 475 °C. (a) TEM bright field; (b) large aperture SAD.

smaller, in the range 150–200 nm. At 850 °C (see Figs 5(a) and 6(a)), the Fe_3B phase is difficult to detect and has been replaced with Fe_2B with possibly some Cr_2B (both phases probably containing large amounts of Cr or Fe plus some Mo), the two expected equilibrium decomposition products of an Fe_3B phase which contains Cr in solution. Although these four phases (α -Fe, χ , Fe_2B , Cr_2B) fulfil the assumed equilibrium condition for a quaternary alloy, there are some distinct lines in the diffraction pattern at this temperature which are not accounted for. These lines correspond most closely to the phase CrB_2 , but it seems unlikely from the phase diagrams that this phase could form at this high temperature. In any event, the phase composition at 850 °C cannot be regarded as fully equilibrated, so that it would be necessary to go to even higher temperatures in order to achieve full phase equilibrium.

Phase development in the Cu-bearing alloy is much different. The α -Fe phase is the first to appear, at 400 °C, and remains the only crystalline phase after heat treatment at temperatures up to 600 °C (Fig. 3).

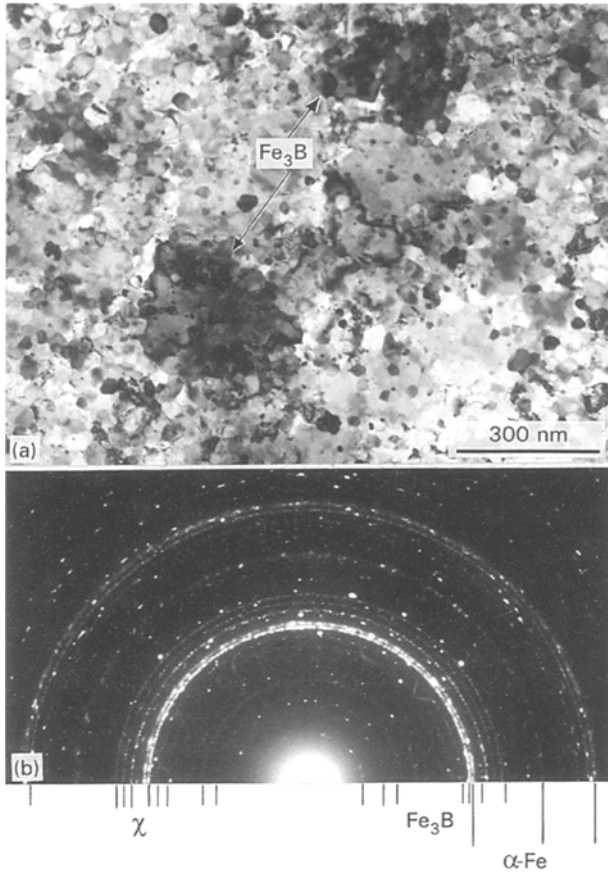


Figure 2 Base alloy, 1 h at 550 °C. (a) TEM bright field; (b) large aperture SAD. Some prominent reflections of the principal phases are marked.

There is no evidence of Fe_3B at any temperature. At 650 °C, Cr_2B precipitates, and at 700 °C there is some suggestion of the χ phase, but identification is uncertain (Fig. 4). By 850 °C the microstructure closely resembles that of the Cu-free alloy (Fig. 5), and the diffraction patterns are very similar (Fig. 6). It is not clear in this case that Fe_2B has formed, though it may be present in lesser amounts, and again one or two unidentified phases appear to be present. There is no diffraction evidence for Cu precipitation at any of the heat treating temperatures.

Since $\alpha\text{-Fe}$ is the predominant phase at all temperatures for the Cu bearing alloy, one may represent the grain growth by measuring the largest grains found at each temperature. This is done in Fig. 7. Two stages appear, one up to approximately 590 °C ($0.65 T_m$) with an activation energy of 33 kcal mol⁻¹, the other above 590 °C with an activation energy of 144 kcal mol⁻¹. Since Cr_2B does not appear below a heat-treating temperature of 650 °C, this dividing temperature is 50–100 °C below the temperature of full crystallization; however, α -grain impingement may begin to occur around 600 °C, affecting the grain growth process.

4. Discussion

The effect of the copper addition on the phase development and grain size in this alloy is most marked below 775 °C. At the lowest temperatures Cu appears to promote precipitation of the b.c.c. α -phase and to

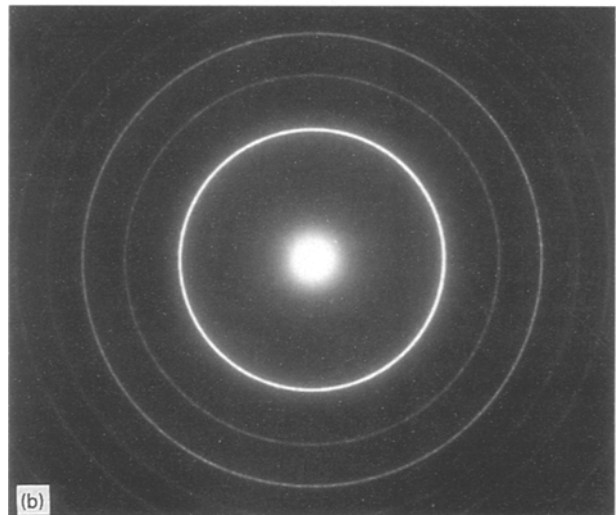
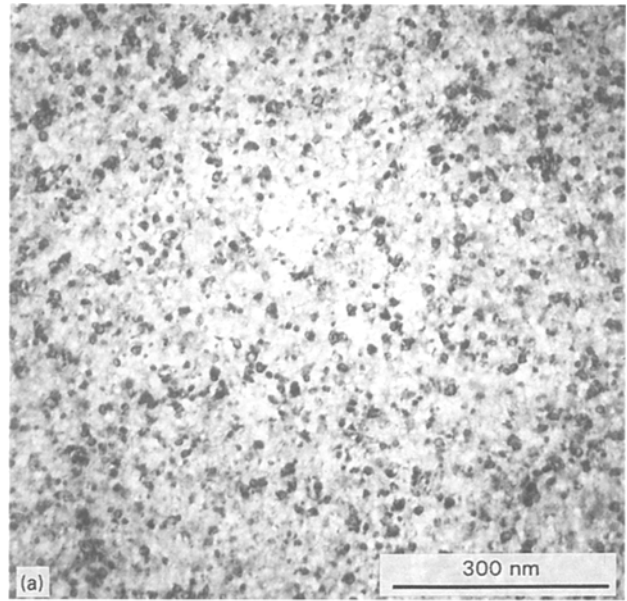


Figure 3 Cu bearing alloy, 1 h at 600 °C. (a) TEM bright field; (b) large aperture SAD.

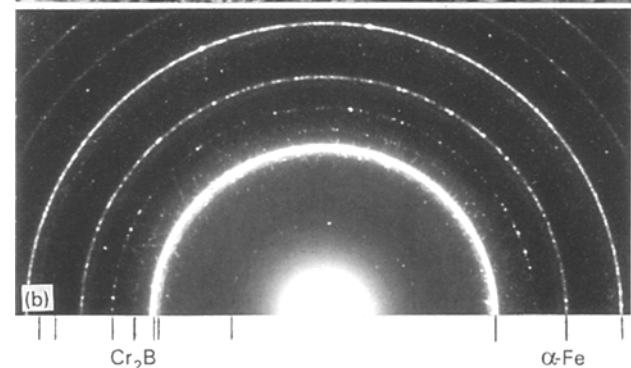
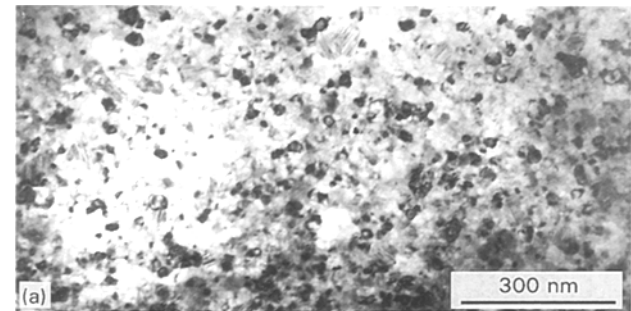


Figure 4 Cu bearing alloy, 1 h at 700 °C. (a) TEM bright field; (b) large aperture SAD.

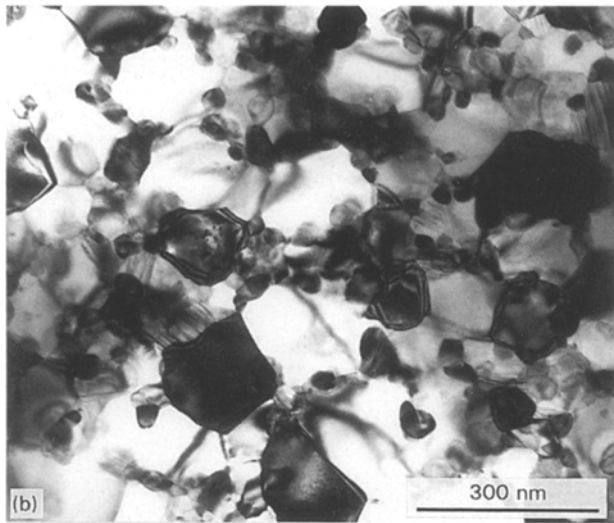
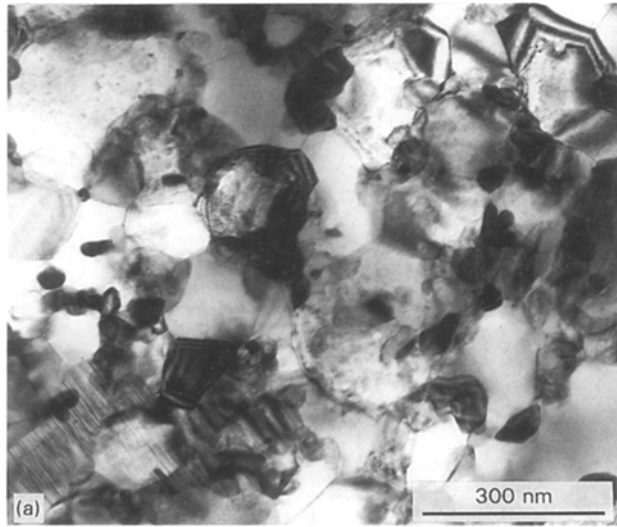


Figure 5 TEM bright field; (a) base alloy; (b) Cu bearing alloy; both 1 h at 850 °C.

inhibit the formation of the Fe–Cr–Mo χ phase. Precipitation of the α -phase is observed in the Cu-bearing alloy at 400 °C, at which temperature the base alloy remains amorphous. The χ phase is the first to appear in the base alloy, at 475 °C, while α -Fe is found at 550 °C and above. These results are in qualitative agreement with findings for a Fe–Si–B alloy [17] where Ag and most transition metal additions raised the temperature of the first crystallization step, but Cu sharply lowered this temperature. There have not been any EXAFS measurements for our alloy to determine if small f.c.c. Cu clusters form first and catalyse α -Fe precipitation, as previously seen for Fe–Si–B based alloys [7].

At intermediate temperatures, the presence of Cu completely suppresses the metastable Fe₃B phase in favour of Cr₂B. Since the Fe₃B grains in the Cu-free alloy are relatively large, while the Cr₂B grains are small, there is a significant difference in grain size between the two alloys in the 550 to 700 °C temperature range. By 850 °C the grain size and phase mixture are very similar in both.

While no evidence was seen of a residual amorphous phase in the Cu-bearing alloy when it was heat

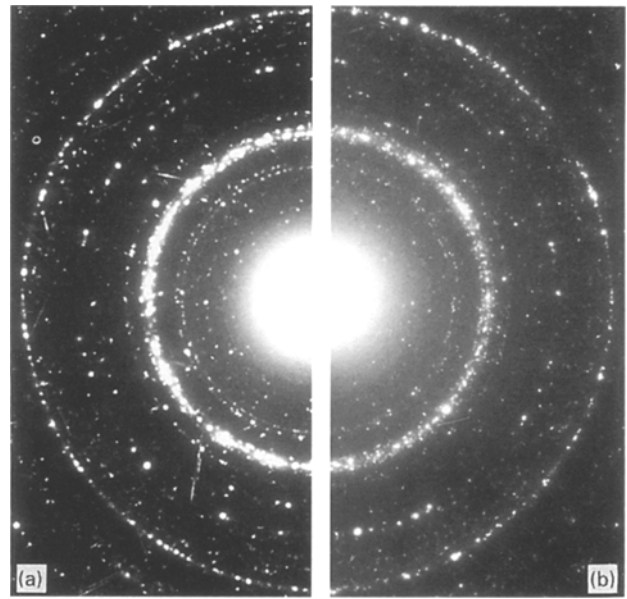


Figure 6 SAD patterns; (a) base alloy; (b) Cu bearing alloy; both 1 h at 850 °C.

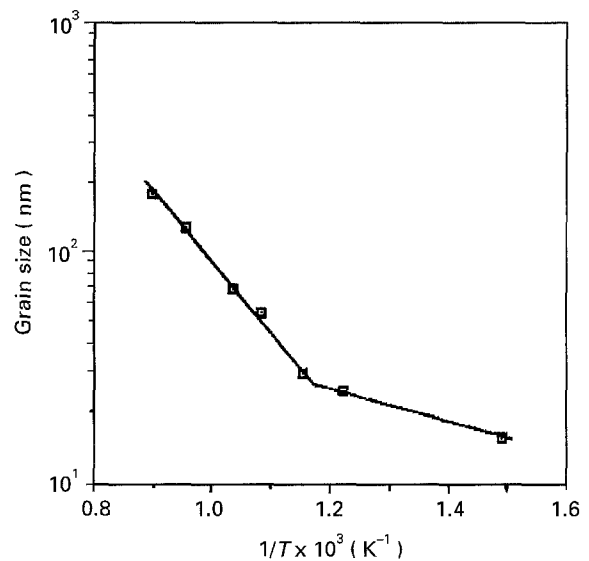


Figure 7 Average size of the largest grains in the Cu bearing alloy versus reciprocal temperature.

treated at temperatures of 550 °C and higher, results of others on alloys in which nanocrystalline α -Fe is the only crystalline phase formed during heat treatment suggests that a film of amorphous phase probably separates the α -Fe grains when the alloy is heat treated at 550 and 600 °C. Such a film would not permit the grain boundary sliding which is necessary for superplastic flow, so low deformation rates would be expected at these temperatures. At temperatures of 650 °C and above, where additional crystalline phases are seen, the amorphous phase is likely to have disappeared, and rapid flow may be possible. After heat treatment at 600 °C, the Cu containing alloy had a maximum grain size of just over 50 nm, while the base alloy had Fe₃B grains approaching 0.5 μ m in diameter. Since grain boundary creep rates increase as the inverse square or cube of the grain diameters, one might see creep rates 100 times greater in the Cu

containing alloy at this temperature. Such an increase could make consolidation of powders or flake possible at reasonable rates with moderate die pressures.

The ribbons of both alloys are brittle after all heat treatments, so consolidates would require further heat treatment to improve toughness, but good physical properties should be attainable. The addition of 1% of Cu has now been shown to substantially refine the crystallized microstructure of three different types of amorphous alloys containing Fe and B, and it seems most likely that similar refinement could be achieved with many additional alloys. This would appear to be an attractive approach to producing fine-grained structural alloys.

References

1. Y. YOSHIZAWA, S. OGUMA and K. YAMAUCHI, *J. Appl. Phys.* **64** (1988) 6044.
2. T. MASUMOTO, A. INOUE, Y. HAKAKAWA, M. OGUCHI and N. YANO, Japanese Patent No. 61-41733 (1986) (in Japanese).
3. Y. YOSHIZAWA and K. YAMAUCHI, *Mater. Trans., JIM* **31** (1990) 307.
4. Y. YOSHIZAWA and K. YAMAUCHI, *Mater. Sci. Eng.*, **A113** (1991) 176.
5. K. SUZUKI, M. KIKUCHI, A. MAKINO, A. INOUE, and T. MASUMOTO, *Mater. Trans., JIM* **31** (1991) 961.
6. K. HONO, AJ.-L. LI, Y. UEKI, A. INOUE, and T. SAKURAI, *Appl. Surf. Sci.* **67** (1993) 398.
7. J. D. AYERS, V.G. HARRIS, J.A. SPRAGUE, and W. T. ELAM, *Appl. Phys. Lett.* **64** (1994) 974.
8. O.D. SHERBY and J. WADSWORTH, *Prog. Mater. Sci.* **33** (1989) 169.
9. R. RAY, *J. Mater. Sci. Lett.* **16** (1981) 2924, 2927.
10. *Metals Handbook*, vol. 8, (ASM, Metals Park, OH, 1973) p. 421.
11. M. L. BORLERA and G. PRADELLI, *Metal. Ital.* **65** (1973) 421.
12. H. HASCHKE, H. NOWOTNY, and P. BENESOVSKY, *Monat. Chem.* **97** (1966) 1459.
13. E. I. GLADYSHEVSKII, T. F. FEDEROV, YU. B. KUZ'MA and R.V. SKOLOZDRA, *Poroshpovaya Metallurgiya, Eng. Trans.* **55** (1966) 305.
14. YU. B. KUZ'MA, V. S. TELEGUS and D. A. KOVALYK, *ibid.* **77** (1969) 403.
15. Y. KAHN, E. KNELLER and M. SOSTARICH, *Z. Metallkde.* **73** (1982) 624.
16. J. L. WALTER, S. F. BARTRAM and R. R. RUSSELL, *Met. Trans.* **9A** (1978) 803.
17. S. BUDUROV, T. SPASSOV, G. STEPHANI, S. ROTH and M. REIBOLD, *Mat. Sci. Eng.* **97** (1988) 361.

Received 30 June 1994
and accepted 11 May 1995